

# MEASUREMENT AND QUANTIFICATION OF A SEDIMENTATION BUDGET FOR A RESERVOIR WITH REGULAR FLUSHING

MARGARETA B. JANSSON\* AND ULF ERLINGSSON

*AB Hydroconsult, Drottninggatan 7, S-753 10 Uppsala, Sweden*

## ABSTRACT

This paper provides a case study of successful removal of reservoir sediment by empty flushing. The main aim of this study was to determine: (i) sediment inflow to the Cachí reservoir; (ii) the pattern and rate of deposition in the reservoir; (iii) the erosion within the reservoir during flushing; and (iv) sediment outflow at a downstream hydrological station during flushing. The results are integrated as a sediment budget for the reservoir. The drainage basin of the Cachí reservoir in Costa Rica is 785 km<sup>2</sup>.

The sediment budget for the period between two flushings indicates a sediment inflow to the reservoir of *c.* 930000 tonnes and a net accumulation of *c.* 133000 tonnes, or 14.3% of the sediment inflow. The sediment throughflow was also *c.* 133000 tonnes up to the erosion phase of the flushing, and the outflow during flushing including bed load was 663000 tonnes, i.e. 71.4% of the sediment inflow. Thus, the flushing of the reservoir was highly effective in releasing sediment.

The balance of the sediment budget makes it probable that the major components of the sediment budget are of the right order of magnitude. The main principle to obtain correct sediment loads by the rating-curve technique was to collect sediment data from a large number of storm events at equal time intervals during rising and falling stages. This was achieved by turbidimeter recordings. Because of the wide scatter of data, sediment rating curves were developed on mean sediment loads in discharge classes to avoid the bias of log regressions.

The trap efficiency and sediment throughflow were determined with Sundborg's physically based sedimentation model. The throughflow amounted to 20% of the suspended sediment inflow, which compares well with the empirical budget. The depositional pattern in the Cachí reservoir was surveyed with side-scan sonar, repeated echo-soundings, and by excavating pits in deposits when the reservoir was empty. Deposition occurred mainly in the old river channel, indicating that the major part of the sediment is transported by density currents.

The volume of eroded material in the reservoir during scour valve release was estimated by echo-soundings before and after the flushing. Dry bulk density of the reservoir deposits was determined by X-ray radiographic and densitometric analysis. The radiographic analyses indicated a dry bulk density of 0.4 g cm<sup>-3</sup> of the loose material in the thalweg, and 0.7 g cm<sup>-3</sup> of the whole deposition depth on the terraces. Copyright © 2000 John Wiley & Sons, Ltd.

KEY WORDS: bathymetric survey; Costa Rica; density currents; depth survey; reservoir flushing; reservoir sedimentation; sediment budget; sediment load; sediment throughflow; trap efficiency

## INTRODUCTION

The Cachí hydroelectric power plant went into production in 1967, but by 1973 the water that was entering the turbines was so turbid on occasions that it affected operations. Pre-hydropower generation studies had not foreseen the flow and depositional conditions causing these problems and the amount of sediment entering the reservoir was greatly underestimated.

The institution in Costa Rica operating the reservoir, Instituto Costarricense de Electricidad (ICE), was forced to flush the reservoir in 1973 to release part of the accumulated sediments. Flushings were thereafter performed 14 times in 18 years. During the flushings, frequent water samples were taken at a gauging station *c.* 10 km downstream of the reservoir to calculate the flushed load.

\* Correspondence to: AB Hydroconsult, Drottninggatan 7, S-753 10 Uppsala, Sweden.  
E-mail: marg.jansson@uppsala.mail.telia.com

ICE used widely accepted methods to measure and calculate sediment transport to the reservoir. The need for further studies of the Cachí reservoir became evident when analyses of 15 years of sediment concentrations indicated that the calculated sediment outflow was three to four times higher than the sediment inflow. There had to be a major error in the methods, since it was obvious that there could be no significant net erosion of the pre-reservoir deposits. Since there existed plans for further development of the Reventazón River, ICE decided to perform detailed investigations of the Cachí reservoir concerning sediment inflow and deposition conditions, in order to find the reasons for the disagreement, and to obtain appropriate knowledge for the future operation of the reservoir.

The study was carried out as a joint Swedish–Costa Rican investigation project, and was reported in English and in Spanish (Jansson and Rodríguez, 1992; Rodríguez and Jansson, 1992). The aims of the research were primarily to calculate the sediment inflow accurately; to investigate the pattern of sediment deposition in the reservoir and the flow conditions causing the sedimentation pattern; the trap efficiency and throughflow; the pattern of sediment release within the reservoir during the flushing; and the mass of sediment outflow during flushing. The flow and sedimentation pattern of the Cachí reservoir had to be investigated to understand the pattern of sediment release during flushing. Moreover, it was necessary to make a reservoir sediment budget for quantification of the effectiveness of the flushing flows to release sediment, and for determining the long-term sedimentation of the reservoir and its economic consequences.

## BACKGROUND OF RESERVOIR SEDIMENTATION

The main principles and concepts of sedimentation in reservoirs of significance to the conditions in the Cachí reservoir will be briefly outlined below. The principles of sedimentation are covered in detail in Bruk (1985), Hydroconsult (1995a), and Morris and Fan (1997). Morris and Fan (1997) also review modelling of sediment transport and deposition, and describe case studies of sedimentation, sediment routing and removal of sediment by flushing. The intention here is to give a general background to sedimentation processes of special importance for this study.

### *Processes*

*Delta growth.* Sand and coarser fractions are mostly transported as bed load. Much of the coarse material is deposited in a delta, close to the actual water level. The variations in thickness of this accumulation thus depend on the water-level variations in the reservoir, especially during the season with the largest inflow of bed load. Suspended sediment also accumulates in the delta area. Moreover, there is some aggradation within the backwater region of the reservoir.

*Inflow conditions and density currents.* Suspended sediment is carried into the reservoir with the inflowing water. If there is no or a very small density difference between the inflowing water and the reservoir water, the mixing of the waters is facilitated and the river water spreads throughout the reservoir. Depending on the density of the inflowing water relative to that already in the reservoir, it may flow as overflow (at the surface), as underflow (along the bottom), or as interflow (at an intermediate depth). The density varies with temperature, sediment concentration, and salinity.

Even rather small temperature differences cause considerable density differences at temperatures between 20°C and 30°C, which is a normal temperature range in tropical waters. A temperature difference of 1°C at a water temperature of 25°C results in a density difference of  $0.00025 \text{ g cm}^{-3}$ , which corresponds to a difference in suspended sediment concentration of  $400 \text{ mg L}^{-1}$  (cf. Axelsson, 1967; Sundborg, 1992a). The formation of density currents is more fully described in Hydroconsult (1995a,b).

If the inflowing water is considerably denser than the reservoir water, a density current will result, provided that the reservoir is deep enough. The distance of travel of the density current depends on the morphology of the bottom, and the magnitude and nature of the density difference.

A turbidity current is a density current in which high sediment concentration constitutes the main cause of the density difference. In the case of the Cachí reservoir there is a combination of temperature and

sediment concentration differences that causes turbidity currents. Turbidity currents carry sediments through the reservoir along the steepest slope. However, the persistence and progression of turbidity currents is affected by the settling process, and the currents dissipate at times through turbulent water exchange.

#### *Effects on hydropower generation*

The processes of sediment transport and sedimentation within a reservoir may have a detrimental effect on the operation of the hydropower plant in several ways, which are summarized below.

*Loss of active storage.* The trap efficiency is generally well over 50%. Deposition can occur both in the active storage zone, and in the dead storage zone where it does not affect the useful volume. While it is desirable to get as much of the sediment inflow as possible to pass the lowest regulation level of the reservoir down to the dead storage zone, delta growth almost exclusively takes place in the active storage zone, and is thus especially harmful.

*Turbid water reaching the turbines.* If sediments reach the turbine blades, these will gradually wear down and lose efficiency. In the case of turbidity currents, suspended sediments may be carried a long distance and settle near the dam. This deposition gradually elevates the bottom and raises the turbidity currents, creating high concentrations of sediment in the water close to the intake, although the water at the surface above the intake may be quite clear.

#### *Mitigation by flushing*

Flushing is most suited for relatively small reservoirs, and in climates with a marked difference between dry and wet season (White, 1990). A pre-requisite for flushing is that there is a bottom outlet (scour valve) in the dam through which the water and the sediments can be evacuated. A detailed presentation of procedures and features of empty (or free-flow) flushing, and pressure (or drawdown) flushing techniques, is found in Morris and Fan (1997). The flushing procedure used in the Cachí reservoir is described below.

Flushing cannot be expected to erode much of the delta deposits, but it is very efficient in eroding the deep channel and in removing soft sediments from the neighbourhood of the scour valve. Thus, unfortunately, flushing is more efficient in the dead storage than in the active storage. In the long term, however, repeated flushings indirectly decrease live storage deposition, since they favour a morphology that stimulates density current sediment transport and sediment release.

The cost of a flushing is high, about 0.5 million US\$ per day in the Cachí case, because of loss of energy production until the reservoir is filled to the lowest regulation level. Moreover, very large concentrations of sediment are brought down-river, where adverse effects on both the environment and technical installations must be anticipated.

It is essential to determine the minimum flushing frequency that would not endanger the long-term economy of the investment. Environmental factors must also be considered. The downstream sedimentological effects of the Cachí flushings have been studied in a separate project (Brandt *et al.*, 1995; Brandt, 1999).

## THE STUDY AREA

#### *Geographical setting*

The Cachí reservoir is located on the Reventazón River draining to the Atlantic side of the Talamanca mountain range in Costa Rica (Figure 1). The Navarro River, a major tributary, enters the main Reventazón River at some distance upstream of the reservoir. Before the junction with the Reventazón there is a gauging station, La Troya, in a straight river reach about 3.2 km from the reservoir (Figure 1). Mean annual water discharge at La Troya is  $8.5 \text{ m}^3 \text{ s}^{-1}$  (1971–1990). The maximum discharge of  $340 \text{ m}^3 \text{ s}^{-1}$  was recorded in 1975. There is another gauging station on the Reventazón River, Palomo, also in a

straight river reach about 5 km from the reservoir (Figure 1). Some distance downstream of Palomo the river is braiding. Mean annual water discharge at Palomo is  $34.4 \text{ m}^3 \text{ s}^{-1}$  (1971–1990). The maximum recorded instantaneous discharge of  $593 \text{ m}^3 \text{ s}^{-1}$  occurred in 1986.

The drainage area is  $785 \text{ km}^2$  at the Cachí dam, and  $877 \text{ km}^2$  at the gauging station El Congo about 10 km downstream of the reservoir. The river upstream of Palomo reaches a maximum elevation of about 3300 m a.s.l., and the basin is mainly covered by mountain rainforest. Close to the Palomo station, there are extensive coffee plantations. Land use is different in the river basin upstream of La Troya on the slopes of the Irazú volcano, with a maximum elevation of 3432 m a.s.l. Vegetables, such as potatoes, onions, carrots and beans, as well as pasture for dairy cattle, are predominant there.

Mean annual precipitation varies from about 1500 mm on the southern slopes of the Irazú volcano, to about 8000 mm (8 m) in an area along the Reventazón River around 2000 m a.s.l. The precipitation distribution can be explained by climatic and topographic conditions. The Reventazón basin has a

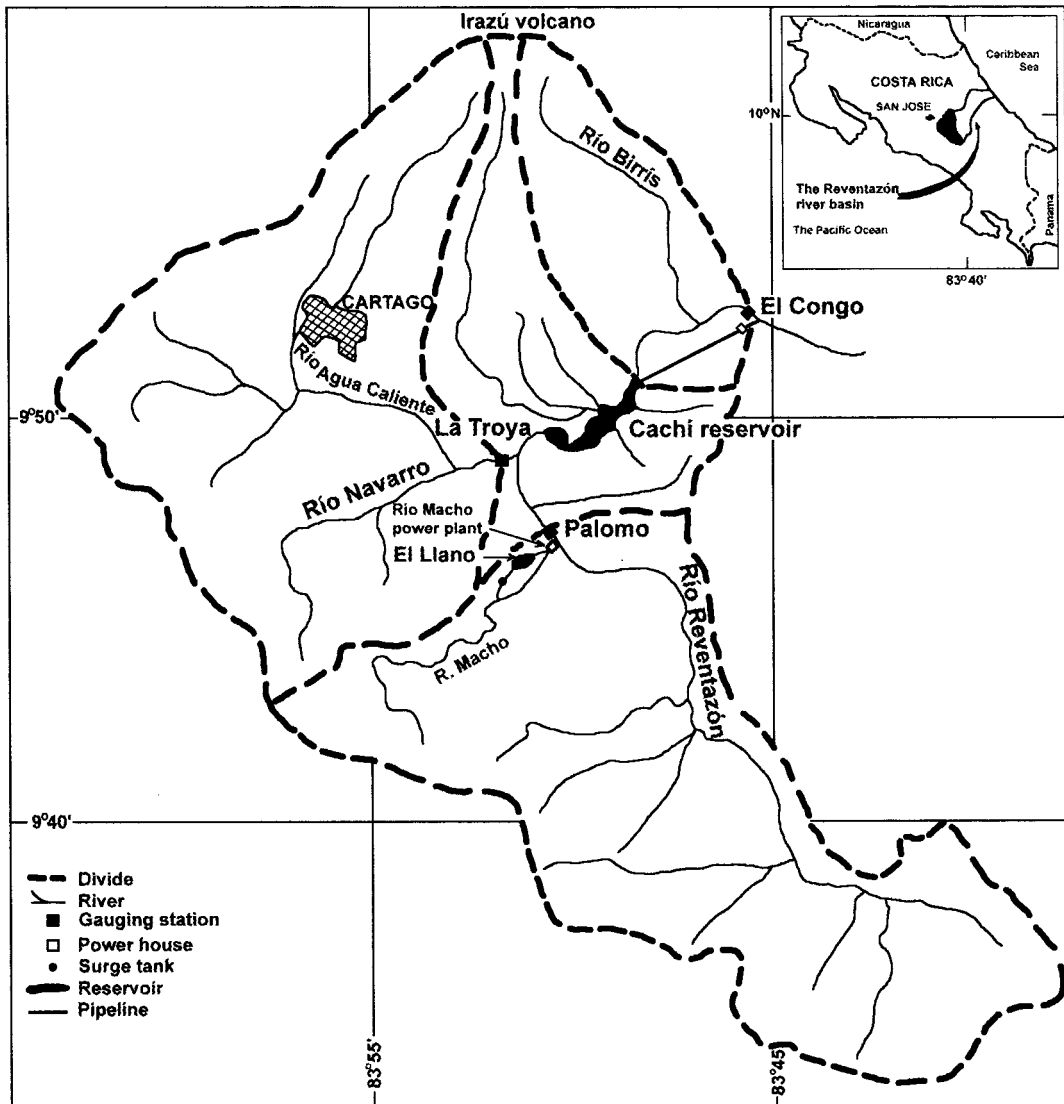


Figure 1. The Reventazón River basin upstream of the gauging station El Congo. During the flushing period the sediment outflow is measured at El Congo

tropical rainforest climate, and is dominated by trade winds from the northeast. The trade winds are especially strong from December to April. During this season outbreaks of cold air, known as 'Nortes', sometimes reach the Caribbean Sea, pick up humidity and heat during the passage of the sea, and produce persistent rains on the windward side of the mountains. During the rainier season, which lasts from May to November, the basin is affected by the Intertropical Convergence Zone, and short-lasting but heavy precipitation is caused by convection.

The above mentioned characteristics of the Reventazón River basin contribute to high gross erosion. The tropical climate with high intensity rains, agricultural land use, and steep terrain combine to make erosion high. Erosion from plots on the slopes of the Irazú volcano during the four rainiest months in 1985–1986 amounted to *c.* 14200 tonnes km<sup>-2</sup> on a 66% slope, 1400 tonnes km<sup>-2</sup> on a 51% slope, 4400 tonnes km<sup>-2</sup> on a 9% slope (calculated from table 15 in Cortes *et al.*, 1987). Moreover, there are frequent slumps and landslides along the rivers. The net erosion, that is to say the mean annual sediment yield, at Cachí calculated in this study for a 10-year period was 1030 tonnes km<sup>-2</sup>.

#### *The Cachí dam and reservoir*

The reservoir had a maximum area of 3.2 km<sup>2</sup> when constructed, and a volume of 54 × 10<sup>6</sup> m<sup>3</sup>. The upper storage level is at 990 m a.s.l., the intake is at 936 m, the minimum generation level is at 960 m, and a bottom outlet is located at 921.5 m. The height of the concrete arch dam is 76 m, and its length 184 m. The maximum water discharge through the turbines is 54 m<sup>3</sup> s<sup>-1</sup>, and the installed capacity is 100.8 MW.

The reservoir is composed of one upper basin, characterized by delta accumulation, and one main basin, separated by a narrow part (Figure 2). The section closest to the dam is a deep V-shaped gorge. More than half of the main basin has a morphology with a thalweg and terraces at various elevations on both sides of the thalweg. The channel here has steep slopes between 5 and 10 m deep, and is between 50 and 100 m wide. The terraces generally slope gently away from the thalweg (see Jansson and Rodríguez, 1992, or Rodríguez and Jansson, 1992, plates I–IV).

### INVESTIGATION OBJECTIVE AND STRATEGY

This study was initiated to obtain knowledge of the sediment transport and sedimentation processes in the Reventazón River and the Cachí reservoir, and primarily to find answers to the following questions:

- How large is the suspended sediment inflow, and how much sediment goes through the reservoir?
- How much bed load reaches the reservoir?
- What is the spatial distribution of sedimentation within the reservoir?
- What are the flow conditions within the reservoir, and what consequences do they have?
- How much material is eroded in the reservoir during flushing, and from where?

The methods used, and their purposes, are indicated in Table I.

More detailed descriptions of the methods, presentation of basic data and calculations, and uncertainty analysis, are found under the headings: sediment inflow, sedimentation in the reservoir, reservoir erosion during flushing, and sediment outflow during flushing. The final analysis and discussion of the results are then presented, in which flow conditions, throughflow and depositional pattern and the sediment budget of the reservoir are in focus.

### SEDIMENT INFLOW

The sediment inflow to the Cachí reservoir for the period September 16, 1989 to October 13, 1990 was determined from measurements at the stations of La Troya and Palomo. An accepted sampling procedure by national hydrological authorities in many countries is to take water samples at a fixed hour during the day, normally in the mornings. This was also done in Costa Rica. Water samples had been taken for 17

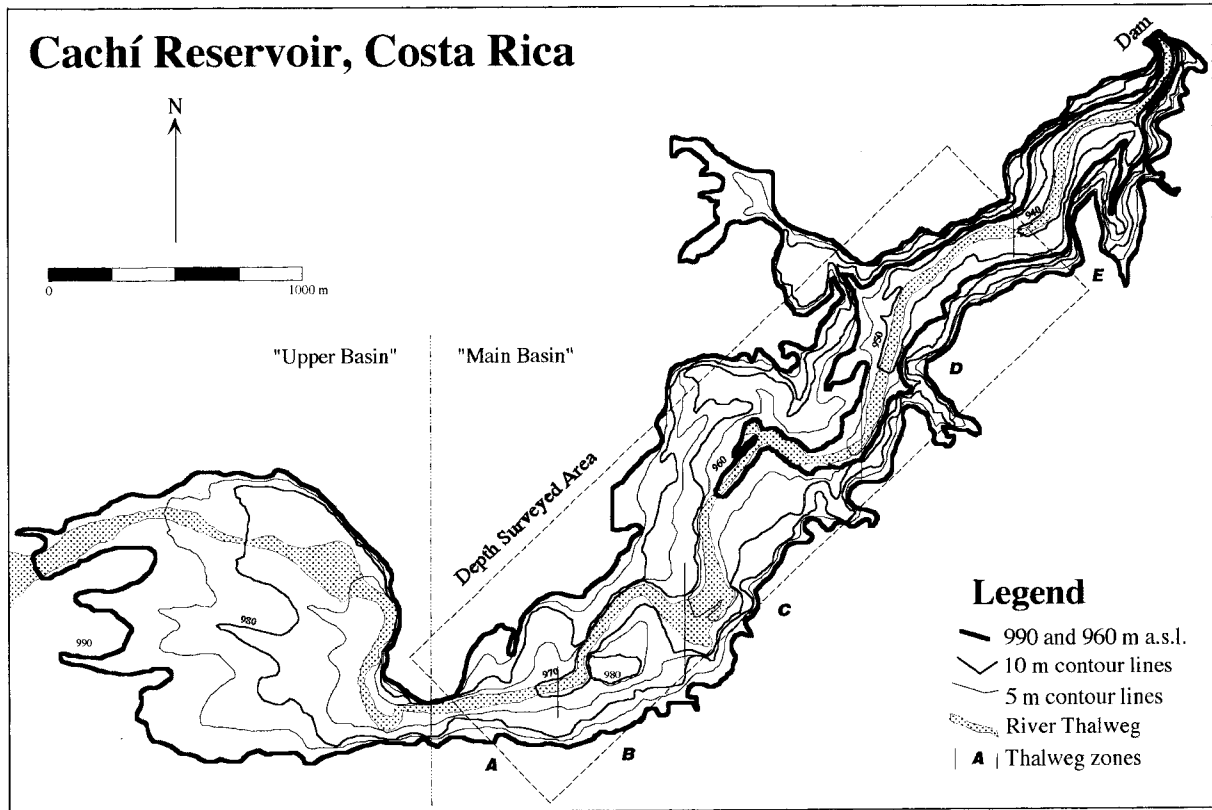


Figure 2. The Cachí reservoir, based on mapping before the reservoir was filled. The upper storage level is 990 m a.s.l., and the lowest generation level is 960 m a.s.l. The reservoir is distinctly separated in an upper, and a main, basin. The repeated depth surveys were made in parallel lines across the reservoir with 100 m intervals. The deep river thalweg is the area with the highest sedimentation

years at La Troya and Palomo. This sampling strategy was assumed to be the main cause of previous erroneous sediment inflow calculations.

The water sampling strategy chosen for this study was based on the concept that most of the sediment

Table I. Methods of measurement and analysis used in the present study

Method	Purpose
Turbidimeter measurements, water sampling	To accurately determine the suspended sediment inflow, and sediment outflow during flushing
Side-scan sonar, sub-bottom profiler, grab sampler	To map the surface sediments in the reservoir
X-raying of sediment cores, and computer analysis of the films	To determine the stratigraphy, dry bulk density, and sediment consolidation
Photographing from a fixed high point at known water levels while the reservoir is gradually emptied	To map the delta area, and calculate the accumulation by comparing the resulting map with the original topographical map
Depth surveys before and after the flushing	To map the amount and spatial distribution of erosion in the reservoir during a flushing
Excavating pits in reservoir deposits when the reservoir is empty	To measure total sediment accumulation, and determine the long-term average deposition rate on terraces
Mathematical modelling	To calculate sedimentation rate and throughflow

is transported during high-water events, which therefore must be sampled intensively. Measurement with turbidimeters was adopted as a method to reach the goal of obtaining data from a sufficient number of high-water events. The turbidity values were converted to sediment concentrations using relationships between the turbidity values and measured sediment concentrations in the river. The converted turbidity recordings were used both to calculate load directly, and to develop sediment rating curves.

The limitations of the sediment rating curve technique for sediment load estimations, and procedures to increase the reliability of load calculations, have been discussed in many papers (e.g. Nilsson, 1971; Walling, 1977a,b; Walling and Webb, 1981). It was not until 1985 (Jansson, 1985; Ferguson, 1986) that a correction for the bias inherent in using log regressions for sediment rating curves was introduced, and by this, load estimations improved considerably in accuracy. However, in this study, with a very wide scatter of data, another method is preferable (described below).

Water discharge estimation is also of great significance to get correct load estimations. The discharge rating curves were often checked in the field, and were found satisfactory except for the last days of the calculation period at La Troya, when the cross-section changed in a storm.

The sediment load was formerly calculated with daily mean water discharges and sediment rating curves. In order to get more reliable sediment load data, 5-min time units of discharge were used with the sediment rating curves for load calculations. Water-level charts had to be digitized for that purpose. The 5-min units eliminate the bias that arises when daily discharge values are used in rating curves that are developed with instantaneous sample values.

### *Instruments and installations*

The water sampling was made by the Instituto Costarricense de Electricidad (ICE) using a USD 49 sampler from a cableway. Depth-integrated samples were taken at three profiles and the three samples were analysed separately. The mean value of the three concentrations was calculated.

Hach Surface Scatter 6 turbidimeters were installed at the two gauging stations Palomo and La Troya (Figure 1). The Hach turbidimeter measures the scattered light at a 90° angle (see Jansson, 1992a,c). The instrument calibration is made with formazin in the range of 0–9999 nephelometric turbidity units (NTU). The accuracy is  $\pm 5.0\%$  from 0 to 2000 NTU, and 10.0% above this concentration. The repeatability is 1.0% or  $\pm 0.04$  NTU whichever is greater.

It was found that the intake tube to the instrument easily became clogged with mud and organic material. The intake flow to the instrument should be  $2 \text{ L min}^{-1}$ . Especially at Palomo, there were great problems with coffee shells choking the river intake tube and the inlet tube of the instrument.

A Monitek Clam 52 LE instrument was installed at Palomo and was found to work better because of the wide tube in which the Monitek sensor was fixed. The Monitek instrument is based on a combination of transmitted light and forward scattered light at 12°. The glass tube in front of the lamp and photocells is wiped automatically with a rubber scraper every 15 s (Jansson, 1992a,c). The repeatability is  $\pm 1\%$ .

The data from the instruments were stored in a Campbell CR10 data logger at 5-min intervals. Six momentary measurements were made with intervals of 10 s. The average was calculated and stored in the logger.

The water intake in the river to the turbidimeter is located at a fixed position close to one bank. A Wacker ESS 750 submersible pump was installed in a metal well. The water was pumped to a hut located above flooding level. The water passes a trap for air bubbles, subsequently passes the Monitek instrument that is positioned in the water tube, and then passes the intake to the Hach instrument. Sedimentation occurred in the bubble trap and after passing the bubble trap. Therefore, measures were taken to remove this silt from the sedimentation pit with a very small jet of spill water when needed.

### *Data handling*

The water levels were recorded graphically and the water stage curve was digitized using the same time intervals as the turbidity recordings, and was converted to water discharge data with rating curves. The errors introduced in the digitizing are estimated to be insignificant in relation to the resolution of the water stage measurements, and to the overall accuracy. A rough estimate gives  $< 1$  cm in water level as a random error.

Correlation between NTU values and measured suspended sediment concentrations was established in the form of regressions. Two to three regressions, referring to different magnitudes of river sediment concentrations, were established for each station. Means of NTU in concentration intervals were plotted on diagrams together with the regression curves to observe the fit of the regressions. At Palomo, very few water samples had been taken in the river at high turbidity, and Monitek recordings were therefore used to determine a relationship at high concentrations. For details, see Jansson (1992a).

#### *Sediment load calculations*

The aim had been to get continuous turbidity recordings for direct sediment transport calculations during the period between the two reservoir flushings, September 16, 1989 to October 13, 1990. However, the recordings were not continuous during the whole period. Sediment rating curves had to be used when turbidity recordings were missing. At La Troya, only about 2% of the time was missing, but at Palomo about 80% was missing.

Figure 3 illustrates the variations in water discharge and sediment concentration with time for some high-water events at La Troya. The concentration peak often lags behind the discharge peak and appears on the falling limb at La Troya. At Palomo the concentration peak often appears on the rising limb. As can be judged from the different peaks in Figure 3, there is no single relationship between water discharge and sediment concentration. Nevertheless, Figure 3 indicates the data base used for the development of a sediment rating curve at La Troya. The band in the middle of Figure 3 represents the period from September to October for which the load was to be calculated. The periods of the data records used for the sediment rating curve are marked on the same band.

Due to the wide scatter of concentrations and loads for the same water discharges, a special method was used to develop sediment rating curves. By definition, a regression should go through the arithmetic mean of loads for every discharge (Jansson, 1996). It is not feasible to calculate the mean load of each discharge. Therefore the load data were sorted according to water discharges, and were divided into water discharge classes. The arithmetic mean sediment load, and the mean water discharge, was calculated for each discharge class. The mean loads and mean discharges in discharge classes were log-transformed, and linear regressions on the logged mean loads in discharge classes were developed as a sediment rating curve (Figure 4). The de-transformed regressions need not, and should not, be corrected for bias (Helsel and Hirsch, 1992).

At La Troya, the squared correlation coefficient of the regression,  $r^2$ , was 0.96, and the S.D. of the log regression,  $s$ , was 0.14 (Figure 4). The sediment rating curve at Palomo was divided into two regressions, one for discharges  $< 185 \text{ m}^3 \text{ s}^{-1}$  with  $r^2 = 0.99$ , and  $s(\text{log regression}) = 0.12$ , and the other with  $r^2 = 0.86$  and  $s(\text{log regression}) = 0.08$  as indicated in Jansson (1996).

The load at La Troya had to be estimated during the last few days of the calculation period because a big storm washed away the pump house and increased the cross-section, implying that the calculated discharge values were too low. A lump load was added to the load calculated from the gauge levels.

#### *Estimated values from unsampled areas and of bed load*

Sediment inflow from tributaries draining directly into the reservoir was estimated by comparing with erosion conditions in three neighbouring basins, where water sampling had been performed and sediment loads had been calculated. The erosion conditions within the three basins were estimated from field knowledge of slope conditions, maps of geology, soils, and land use, and from comparison of the areas in a potential gross erosion map constructed with the USLE. Sediment yield ( $\text{tonnes km}^{-2}$ ) from the basin with the most similar erosion conditions was used in the calculation of load from the unsampled area.

The bed load inflow is difficult to determine. Empirical relationships between the bed load transport rate and the concentration of suspended material, and the type of material forming the stream channel, indicated a percentage of bed load amounting to 5–12% of the measured suspended load (cf. Lane and Borland, 1951). An average of this was chosen after checking that the grain sizes of the delta were not



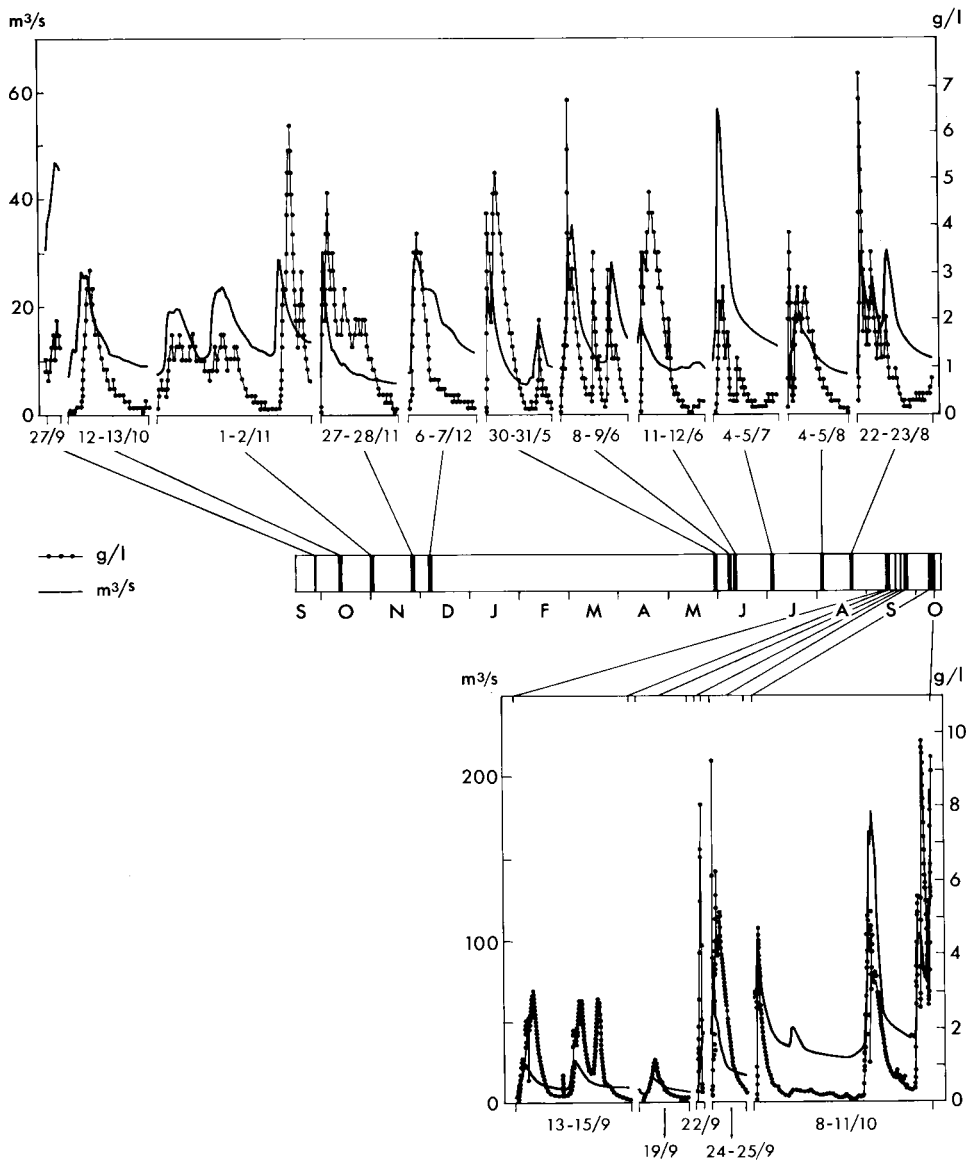


Figure 3. The data base for the development of a sediment rating curve at La Troya. The calculation period between two flushings is indicated in the centre, and the periods when data for the sediment rating curve were collected are also indicated there. Rainfall is lower during December–May

indicative of an unusually high bed-load content. Thus, the bed load was calculated as 8% of the suspended sediment inflow.

### SEDIMENTATION IN THE RESERVOIR

Using different methods an attempt was made to quantify the amount and distribution of sedimentation in the reservoir, both since the last flushing, and since the dam was completed. Part of this information gave the fundamental conditions for the mathematical trapping efficiency model and another part was used to verify the model.

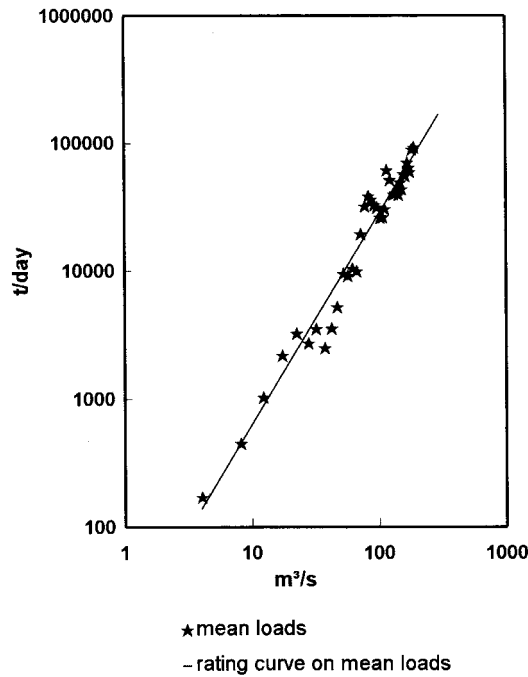


Figure 4. Sediment rating curve at La Troya. The calculated mean loads in discharge classes are indicated. The rating curve is  $L = 14.18Q^{1.645}$ , with  $r^2 = 0.96$ , and  $s(\log \text{ regression}) = 0.14$

#### *Side-scan sonar*

The reservoir was surveyed prior to the flushing with a 105 kHz EG&G Model 260 side-scan sonar and an O.R.E. 14 kHz sub-bottom profiler (described in Erlingsson, 1990, 1992a). Three lines were run lengthways through the main portion of the reservoir, between the narrow part and the dam (Figure 2). The sonographs and profiles were analysed together with the sediment X-ray images (see below), with stereo air photos taken during a previous flushing (Erlingsson, 1992a, plate IV), and with oblique air photos taken during the present flushing. The objective was to qualitatively interpret the spatial pattern of grain-size distribution, sedimentation, and consolidation processes. It was also found that there was a correlation between grain size and back-scatter strength, with stronger echo for material finer than 0.01 mm, in agreement with conclusions by McCann and McCann (1969).

Applying traditional marine geological survey methods in this hydropower reservoir allowed the observation that the sediments on the terraces were acoustically distinct from the sediments in the thalweg, and the conclusion was that this reflected a significantly higher sedimentation rate in the thalweg (Erlingsson, 1992a, p. 107).

#### *X-ray radiography*

Sediment cores for X-ray radiographic analyses were taken with a gravity corer, designed by Axelsson, consisting of rectangular exchangeable coring tubes, which are screwed onto a corer head (cf. Axelsson, 1992a). The corer head is fitted with a valve system that allows unrestricted flow of water through the coring tube both during descent and during penetration into the sediments. The valve closes at the start of retrieval. The coring tubes are rectangular and are made of transparent acrylic glass, which has a small coefficient of absorption of X-rays at low and moderate energy levels (Axelsson, 1992a).

The cores were irradiated together with a seven-stepped aluminium wedge for density calibration. Variations in the film density along the centreline of the radiation images of the sediment cores and the aluminium wedge were recorded by a Joyce-Loebl 3CS microdensitometer. A Thiemer DDM3

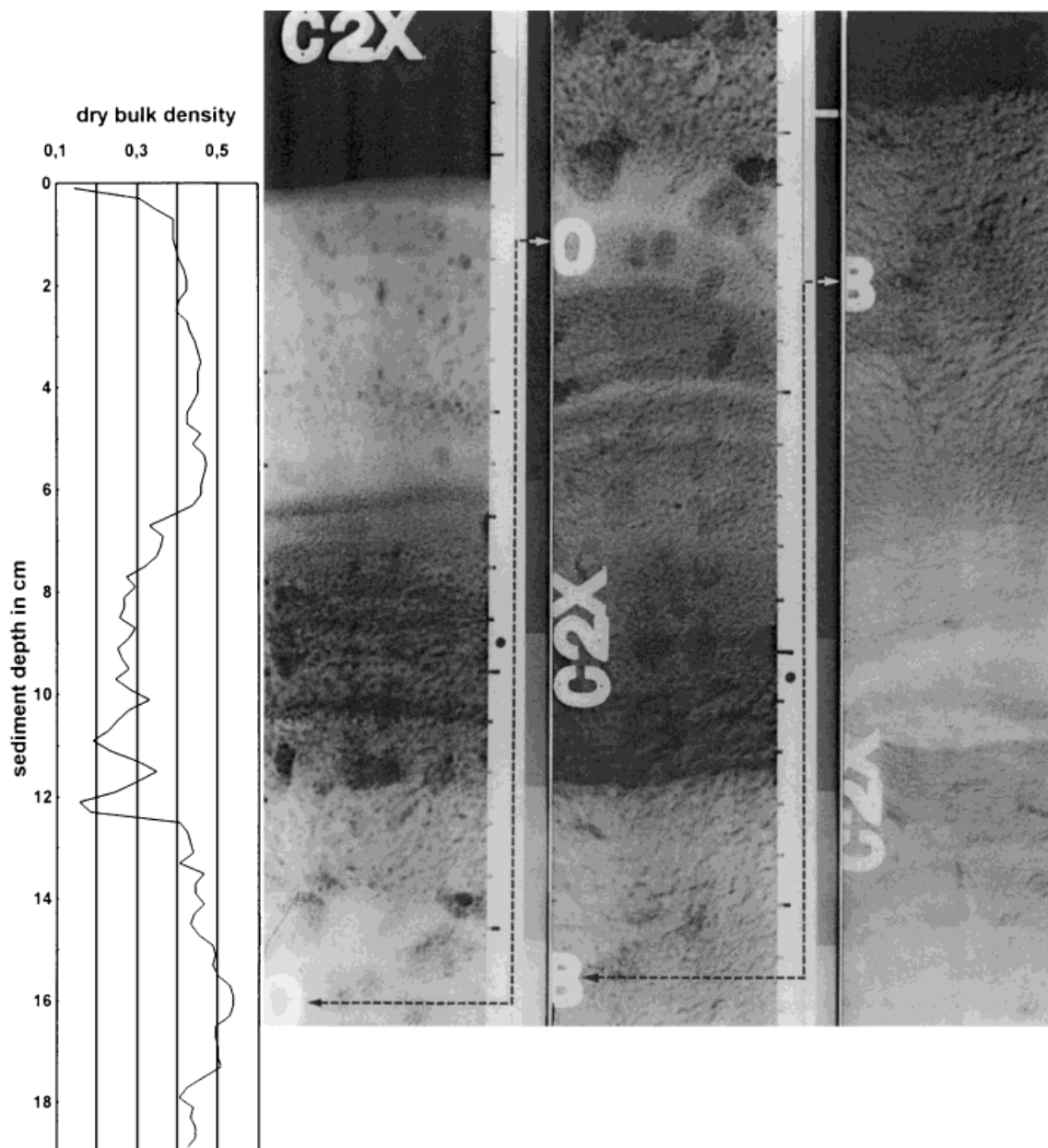


Figure 5. Radiographs of sediment core C2 taken in the thalweg of the Cachí reservoir. The dry bulk density curve is drawn for the 19 uppermost centimetres of the sediment core which is 45 cm. The scale is similar for the curve and the radiograph

transmission densitometer with digital readout was used for manual film density measurements. The optical density values were analysed in the computer program 'XRAY.FOR' (Axelsson and Hårdén, 1987) to calculate, print out, and plot the vertical variations in wet and dry bulk density, water content, porosity, void ratio, effective overburden pressure, the increase of solids with increasing sediment depth, and in plotting sedimentation–compression curves. The X-ray image of a sediment core (no C2) from the thalweg is shown in Figure 5 together with the dry bulk density plot of the uppermost 19 cm.

The X-ray analyses have a resolution of 2 mm in the vertical direction (Axelsson, 1992b). The accuracy of the calculations increases with decreasing density of the deposits. For wet bulk densities lower than 1.20

$\text{g cm}^{-3}$  the S.D. from the true values is generally less than 1% (Axelsson, 1979). For high wet bulk densities, the S.D. can reach 2%.

#### *Delta survey*

About 1 km downstream of the mouth of Río Reventazón there is a narrow section in the reservoir, dividing it into an upper basin and a main basin (Figure 2). Delta deposits have accumulated in the upper basin since the damming of the reservoir. By comparing the contour lines of the original topographic map, with photos taken from a fixed high point at successively lower water levels during the reservoir flushing in 1990, an estimation could be made of the amount of material accumulated within the delta area since the damming of the reservoir (Sundborg, 1992c).

#### *Terrace survey*

Net sediment deposition on the terraces was measured by ICE in 1985 when the reservoir was empty for more than 15 days, and it was possible to map the terraces or flat areas on which sediment in suspension had been deposited. Holes were dug on each terrace down to the pre-reservoir surface, and the depth of the accumulated material was measured. In this manner, knowing the terrace area and the average thickness of deposited material on each terrace, the sediment volume on terraces was obtained. The slopes on which there were no deposits were not taken into account (Ramírez *et al.*, 1992). Net deposition on the terraces was  $53 \text{ mm year}^{-1}$ .

Samples from the sediment surface before flushing were taken with a modified Petersen grab sampler. They were analysed for grain size according to the ASTM-D422 densitometric method, and for organic matter content determined with the loss on ignition method.

#### *Mathematical modelling*

The mathematical sedimentation model developed by Sundborg is based on the physical processes of particle deposition as a function of settling rate and flow conditions (Sundborg, 1992a). The sedimentation rate depends on sediment concentration, settling velocity of the suspended material (grain-size distribution), flow velocity, turbulence, depth of flow, and width of flow. The efficiency of the reservoir to trap suspended sediments can be written as follows (Sundborg, 1992a):

$$T = 100 \left\{ 1 - e^{-\left( \frac{w \cdot \Phi(w) \cdot A_{\text{flow}(D)}}{Q} \right)} \right\}, \quad (1)$$

where  $T$  is 'trap efficiency' which is the percentage of material with a given settling velocity  $w$  that is deposited in the reservoir,  $Q$  is water discharge (or volume of water flowing through the lake per unit of time),  $\Phi(w)$  is the relation between the suspended sediment concentration of particles with a settling velocity  $w$  close to the bed and the mean concentration in the flow.  $A_{\text{flow}(D)}$  is the 'area of active flow', which means the total horizontal area of the active water flow through the reservoir upstream of the dam under any given conditions (the area through the reservoir where the flow is active).

The model can be applied to calculate the sedimentation rate and grain-size distribution as a function of distance downstream in the reservoir, for each selected grain-size distribution and discharge in the inflowing river.

An application of Equation (1) with integration over all water discharges  $Q$  and all settling velocities  $w$  (with the settling velocity distribution determined in samples from the inflowing water) gives the total trapping of material in the reservoir. The 'active flow' areas for density bottom current conditions are much narrower than for other flows. The vertical extent of the density (turbidity) currents was assumed to be *c.* 5 m (see section 'Final Analysis of Results'), and their widths to be equal to the old river gorge (*c.* 100 m). Based on the results of the studies of bottom topography and bottom sediments, it was presumed for the mathematical modelling that roughly 90% of the deposition takes place from turbidity currents, and that about 90% of high water discharges and about 30-50% of the lowest discharges have persistent density currents (Sundborg, 1992a).

A ten-year period of water discharges and sediment inflow, estimated from sediment rating curves, was used for the mathematical modelling calculations (Sundborg, 1992a,b).

The mathematical modelling of sediment deposition was verified using the empirical results, such as the deposition in different parts of the reservoir, and grain-size distribution in the reservoir, thus making possible a reliable estimation of trap efficiency and sediment throughflow and of deposition in the upper basin used in the budget. A predictive application of the model for downstream reservoirs is reported in an investigation by Hydroconsult (1995a).

## RESERVOIR EROSION DURING FLUSHING

The amount of sediment eroded during the reservoir flushing was estimated from repeated depth surveys. This also indirectly revealed features of the depositional pattern.

### *Repeated depth surveys*

*Procedure.* The erosion within the reservoir was measured by taking the difference between two depth surveys, before and after flushing, using a traditional single-beam echo-sounder, a Lowrance X-16, 192 kHz, 45° opening angle. The position was measured with a Geodimeter® 140H total station, measuring bearing and distance to the vessel every second. The information was transmitted to the vessel by means of a radio link. On board, a computer calculated the position in the national grid system and stored the information on disk (Erlingsson, 1992b). The survey was limited to the main basin (Figure 2).

The reservoir was surveyed with cross-profiles perpendicular to the length axis of the reservoir, and with a spacing of 100 m. All cross profiles were digitized and converted to files containing depth versus time. These files were merged with position files, using the time code, into files containing  $[x, y, z]$  data. The resolution of the stored position data was 1 m, and of the depth data 0.01 m.

Following the procedure used by Erlingsson (1992b), all depth values within 100 m<sup>2</sup> (10 × 10 m) grid cells were averaged. For the cells where data existed from both the surveys, the average difference in depth was calculated together with the S.D. There were 542 such cells, the result being a mean value of −0.260 m and a S.D. of ±1.588 m.

*Bias due to the transducer opening angle.* An error source, disregarded in Erlingsson (1992b), is the error due to the opening angle of the transducer, also known as beam width. The argument for neglecting it was that the in-survey and out-survey were performed with the same equipment and under roughly similar conditions, and therefore the error associated with a large opening angle was expected to be identical in the two surveys. However, a systematic difference in water level will introduce a bias.

Defining the actual depth as the vertical distance from the echo-sounder transducer to the bottom, and assuming that the indicated depth is free from other error sources, such as variations in sound velocity, the actual depth for a plane but sloping bottom can be calculated from the indicated depth as follows:

$$d_{\text{actual}} = d_{\text{indicated}} \frac{\sin(90 + \alpha 0.5\vartheta)}{\sin(90 - \alpha)} \quad \alpha \geq 0.5\vartheta, \quad (2)$$

$$d_{\text{actual}} = d_{\text{indicated}} \frac{1}{\sin(90 - \alpha)} \quad \alpha \leq 0.5\vartheta,$$

where  $\alpha$  is the bottom slope angle, and  $\vartheta$  is the opening angle of the transducer. The systematic error is thus a linear function of depth. When, as in this case, the difference in depth between two surveys is sought, an approximate correction can be calculated from the difference in water level and the bottom slope.

The average difference in water level between the two depth surveys was 1.5 m. Since the sailing lines in most cases were perpendicular to the steepest slopes, it was considered reasonable to use the along-track slope in the calculations. Since the error is not a linear function of the slope, a weighted

average was calculated by multiplying the error for each slope angle by the relative frequency of that slope angle. The weighted systematic error, i.e. the bias, was calculated to be  $+0.026$  m. The correction to be made is positive since the water level was lower at the out-survey than at the in-survey.

*Uncertainty estimate.* Since each of the 542 cells mentioned above is a mean of, on average, 2.7 samples, the result is a 'mean of means' with a S.D.  $\sigma = \pm 1.588$  m, and the mean error would have been  $\varepsilon = \pm 0.068$  m if the data had been uncorrelated (epsilon is used here to denote the S.D. of a mean value). As could be expected, a spatial correlation analysis revealed that the erosion data were correlated, with  $r = 0.71$  between adjacent cells. For spatially correlated data the formula for the mean error is (cf. Eriksson, 1972):

$$\varepsilon_c = \sigma \sqrt{\frac{1-r^2}{n}}, \quad (3)$$

which gives  $\varepsilon_c = \pm 0.048$  m. This value represents an approximation of the uncertainty in determining the mean erosion depth.

Erlingsson and Jansson (1999) performed additional erosion calculations by orienting the grid net of 10 m cells differently in relation to the echo-sounding data, and arrived at an erosion value of  $-0.280$  m, after correction for the opening angle bias.

Erlingsson and Jansson (1999) also performed an analysis of the error sources based on equipment, measurement and calculation procedures, and concluded that, altogether, the uncertainty of the erosion depth estimate is  $\varepsilon = \pm 0.045$  m, equivalent to a variation coefficient of 16%. This value includes effects of transducer depth, digitizing errors, position errors, sound velocity variations, the sampling of data with erosion variations, and the increased accuracy due to more sampling and repeated calculations, etc. The largest uncertainty contribution was the manual digitizing process (including horizontal errors), and the sound velocity variations. This is encouraging, as both can be decreased significantly using modern equipment.

#### *Correction for post-flushing deposition*

A correction of the measured erosion had to be made, based on interpretations and conclusions. The measured average erosion value ( $-0.280$  m  $\pm 16\%$ ) is the difference between the two surveys. The timing of the depth surveys in relation to the water level of the reservoir can be seen in Figure 6. The erosion

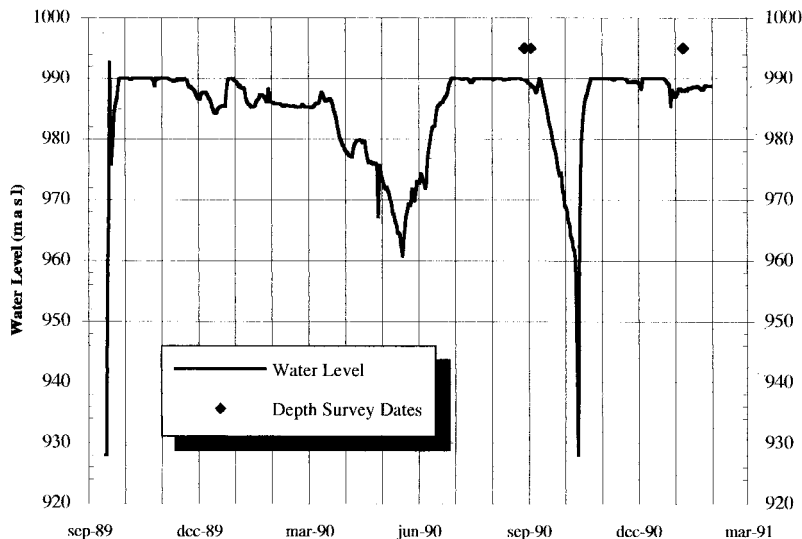


Figure 6. The water-level fluctuations in the reservoir (daily values) from the flushing in September 1989, to the second depth survey in January 1991

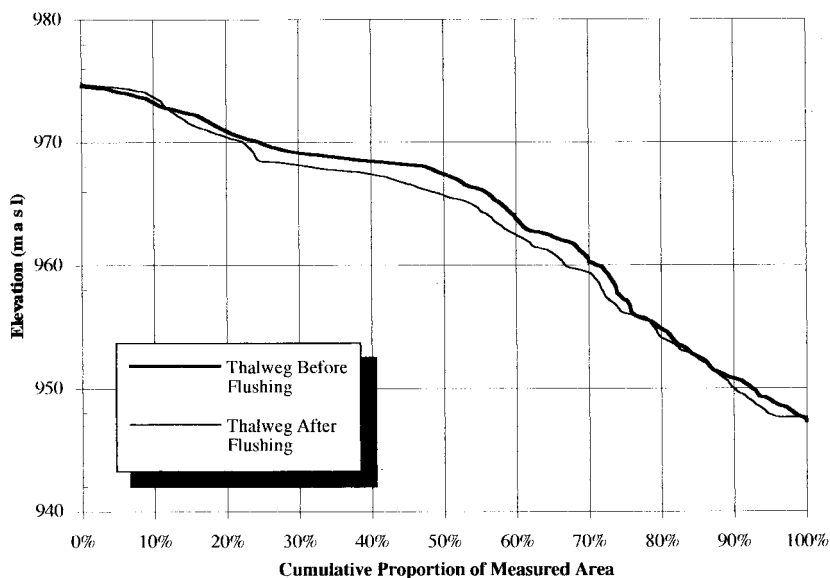


Figure 7. The cumulative distribution of depths in the thalweg within the surveyed area indicated in Figure 2, at the two survey occasions which are indicated in Figure 6. The gentle slope between 25 and 50% corresponds to the stretch where the thalweg is widest (cf. Figure 2). It coincides with some of the largest erosion rates. In the elevation interval 973–975 m, the post-flushing sedimentation during November–December exceeded the amount that was deposited during August–September (cf. Figure 6). The graph is based on a GIS interpolation of the bathymetric data using 1 m cells

of material deposited up to the date of the in-survey, September 4, 1990, was calculated. Thus, the figure required for the sediment budget is the change in depth from the in-survey to the end of the flushing of the reservoir, and not the net change at the time of the out-survey.

The thickness of sediments accumulated from the end of the flushing to the out-survey thus had to be estimated. Based on an analysis of echo-sounding profiles, on an interpolated map of the net erosion in the thalweg (cf. Figure 7), and by analysing water-level data from before and after the flushing (Figure 6), it was estimated that a significant amount of sediment had accumulated in this period. The exact amount is hard to quantify, which is why this becomes the main source of uncertainty in the total erosion estimate.

The estimate made by Erlingsson (1992b) was that 50% should be added. In other words, 0.14 m or one-third of the sediment thickness that was deposited before September 4 and eroded during the flushing, had already been re-deposited at the time of the out-survey. Re-estimations in the thalweg with modern software confirm this conclusion (see below).

The amount to be added obviously cannot be below zero, nor can it realistically be above the measured net erosion of  $-0.28$  m. An uncertainty in post-flushing deposition of 50% is chosen as probably being on the safe side, equivalent to adding an erosion of  $-0.14 \pm 0.07$  m. The total erosion to the end of the flushing thus calculates to  $-0.42$  m, and the uncertainty at the same time increases from  $\pm 16\%$  to  $\pm 20\%$ .

#### *Conversion to volume and mass*

The area of the main part of the reservoir is *c.* 2 km<sup>2</sup> at the upper storage level of 990 m a.s.l. The survey was limited to the area below 985 m a.s.l., about 1.9 km<sup>2</sup>. Furthermore, the stretch closest to the dam was not surveyed, which excludes a further 0.4 km<sup>2</sup>. The surveyed part had thus an area of 1.5 km<sup>2</sup>. Both sedimentation and erosion are expected to be insignificant between 985 and 990 m a.s.l., but are expected to be significant in the thalweg close to the dam. That part was not echo-sounded since the beam width was too large in relation to the dimensions of the gorge.

The area over which to apply the erosion depth of  $-0.42$  m is thus  $1.9$  km<sup>2</sup>, which is a figure with rather good precision (probably about  $\pm 5\%$ ), but to account for the extrapolation from  $1.5$  to  $1.9$  km<sup>2</sup>, an uncertainty value of  $10\%$  was assumed. The volume eroded from the main basin thus calculates to *c.*  $800000$  m<sup>3</sup>, with an uncertainty of *c.*  $\pm 22\%$ .

The results from the X-ray technique indicated that the average dry density of the eroded sediments in the main channel was  $0.4$  tonnes m<sup>-3</sup> (Axelsson, 1992a) and the precision of this figure as the average density of material eroded in channels and on terraces was estimated to be high,  $\pm 10\%$  (Axelsson, personal communication). Multiplying this density by the volume makes *c.*  $320000$  tonnes  $\pm 24\%$  of the total eroded material in the main basin.

#### *Erosion in the thalweg*

The erosion in the thalweg alone was calculated more precisely in a GIS, in an attempt to achieve a spatial image of the distribution of the erosion. By limiting the interpolation to the relatively flat bottom of the channel, a simple inverse-distance interpolation could be made using  $1 \times 1$  m cells. Two separate maps of the sediment surface were thus made, one from each echo-sounding. The net volume change between the two maps was calculated at  $353000$  m<sup>3</sup>. Figure 7 is based on those maps.

The sedimentation after flushing, but before the second depth survey, was estimated by dividing the thalweg into four zones (A–D in Figure 2), plus the fifth, not surveyed part (E), for which the values from zone D were extrapolated. The full calculations are given in Table II.

The estimate of the post-flushing deposition in zones A and B is based on an analysis in Figure 6 of pre- and post-flushing water-level fluctuations, together with the measured erosion depth in each zone (Table II). It was assumed that the total erosion had been largest in zone C. The up-reservoir zones A and B would have been eroded in April to June, and the material deposited in zone C. Based on sonographs and echograms it was concluded that about  $0.4$  m had accumulated in zone C after flushing, and the same in zone D. This value was extrapolated to zone E as well.

Adding the estimated value of deposition from the end of the flushing to the out-survey,  $195000$  m<sup>3</sup>, to the measured erosion of  $353000$  m<sup>3</sup>, the total erosion in the thalweg was calculated at  $548000$  m<sup>3</sup>. As mentioned above, the dry density was found to be about  $0.4$  tonnes m<sup>-3</sup>, and so the total eroded mass in the thalweg would be *c.*  $219000$  tonnes.

No evaluation of uncertainty has been made for this estimate, but from a qualitative estimation it is believed to be at least as accurate as the erosion value for the entire main basin.

## SEDIMENT OUTFLOW DURING FLUSHING

The sediment outflow from the reservoir during the flushing was determined by measuring sediment concentration and water discharge at the El Congo station, and by using turbidity measurements.

#### *The flushing procedure*

The emptying of the Cachí reservoir is done in three phases: the slow evacuation phase, the rapid phase, and the free-flow phase. During the slow phase electricity is still generated, and the water level is lowered  $1$  m every  $24$  h down to the minimum generation level. During the first few days of the slow phase, water is evacuated through the spillways, then by opening the bottom gate for short periods. The rapid phase begins when the water level is near the water intake to the power station, and the scour valve is left open. This phase lasts for about  $5$  h. Finally, there is a free-flow phase, which is when all the dammed water of the reservoir is released, and the river water flows freely through the reservoir.

#### *Measurement and calculation methods*

Depth-integrated water samples were taken from a cableway at El Congo during the flushing (Figure 1). For the slow evacuation phase, the bottom gates were opened for  $0.5$ – $1$  h periods every day, during



Table II. Erosion in the thalweg at the end of flushing. Based on sonographs and echograms it was concluded that about 0.4 m had accumulated in zone C after flushing<sup>a</sup>

Thalweg zone (Figure 2)	Approximate levels (m a.s.l.)	Measured change (m)	Relative area <sup>b</sup> (m <sup>2</sup> )	Measured volume × 1.9 (m <sup>3</sup> )	Estimated deposition (m)	Resulting additional volume (m <sup>3</sup> )
A	973–975	+0.322	21 500	+13 000	0.9	–37 000
B	970–973	–0.622	37 600	–44 000	0.6	–43 000
C	956–970	–1.594	77 600	–235 000	0.4	–59 000
D	947–956	–0.616	46 800	–55 000	0.4	–36 000
E	922–947	–0.6 <sup>a</sup>	27 800	–32 000	0.4	–21 000
Sum			211 300	–353 000		–195 000

<sup>a</sup> The other values were estimated from this. In zone D an echogram showed about 0.5 m of post-flushing accumulation of very soft sediments. The value 0.4 m was considered realistic also for zones D and E. Deposition in zones A and B is based on an analysis of measured erosion depth, and of a water-level drawdown with subsequent erosion in zones A and B.

<sup>b</sup> An estimated value.

<sup>c</sup> This area is derived from the digital map, and it is narrower than the real thalweg area. The interpolations were limited to this area only. To calculate the total volume, each relative area shall be multiplied by 1.9 (to apply for the total thalweg area of approximately 400 000 m<sup>2</sup>).

which altogether 363 depth-integrated water samples were taken in three profiles at El Congo. They were processed in the same way as the samples from the inflow stations, resulting in 121 mean concentrations. The load of a water peak was calculated by ICE by summation of the product of mean water discharge and mean sediment concentration of subsequent sampling occasions, for the whole water peak. For flushing peaks without water sampling, the load was calculated by using the result from the sampled peak nearby in time, in relation to the water volume of the unsampled peak.

During the rapid evacuation phase, water samples were taken about every 15 min at El Congo, as this phase has high sediment discharge. During the free-flow phase, the sediment discharge is lower and water samples were taken every 0.5 h. The load was calculated as for the slow phase, i.e. the mean concentration of two subsequent sampling occasions times the mean discharge times the period of time between the sampling occasions; and summation of the loads for the whole flow phase.

An additional method, introduced for this project, was turbidimeter measurements during the reservoir flushing. A Monitek Clam 52H turbidimeter was installed at El Congo measuring station (Jansson, 1992b). The model 52H utilizes a single light source and three photocells. One photocell measures the transmitted light, a second photocell measures light scattered at a 90° angle to the transmitted path, while a third photocell measures light reflected by the water. This instrument covers a range of concentrations up to 100000 ppm, and the repeatability is  $\pm 2\%$ . The data were stored in a Campbell CR10 logger.

Relationships between water sample concentrations and turbidity recordings were developed. The regression for the rapid phase has  $r^2 = 0.95$  and for the free-flow phase  $r^2 = 0.85$ . These relationships were used to calculate the flushed load from turbidity recordings and digitized stage charts at 5-min intervals.

#### Observations and uncertainties of results

During the slow evacuation phase, short duration discharge peaks of up to  $300 \text{ m}^3 \text{ s}^{-1}$  at El Congo had sediment concentrations of  $1\text{--}2 \text{ g L}^{-1}$ . During the rapid phase, the water discharge reached nearly  $500 \text{ m}^3 \text{ s}^{-1}$  (Figure 8). The highest sediment concentrations of almost  $300 \text{ g L}^{-1}$  appeared at the end of the

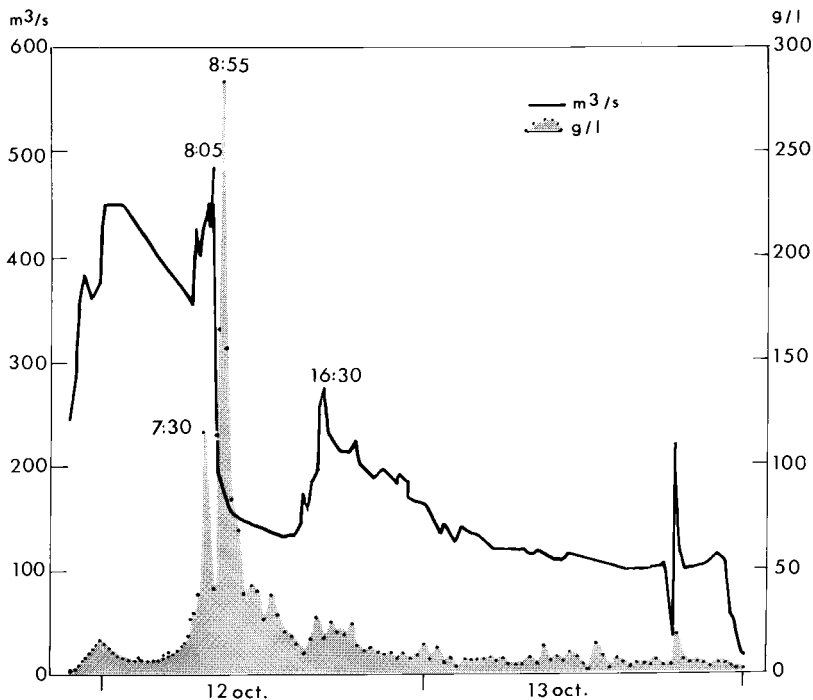


Figure 8. Values of water discharge and water sample sediment concentration during the rapid and free-flow phases of the flushing at El Congo in 1990

rapid phase and the beginning of the free-flow phase, when the remaining high-turbid bottom water in the reservoir was released. High concentration suspensions resembling mudflows were seen in the reservoir close to the dam at the beginning of the free-flow phase. The concentration peak lagged behind the water discharge peak with 50 min at El Congo, located 10 km downstream of the dam and lagged still more at a station further downstream (cf. Heidel, 1956; Hydroconsult, 1995a). This implies an anticlockwise hysteresis loop (cf. Leeks and Newson, 1989). There was a small rise in water discharge at 16:30 h due to rainfall, leading to an increase in sediment transport from the reservoir, and re-suspension of material from the river bed (Figure 8).

The load calculated with water sample data at El Congo was compared with sediment outflow calculated from turbidity recordings during the rapid and free-flow phases. However, the highest concentrations of 150–300 g L<sup>-1</sup> could not be measured by the turbidimeter and for that short period and for a second period, the load was calculated from water sample values. The two regressions between the turbidity data and sediment concentrations were used, one for the rapid phase and one for the free-flow phase. The load calculated with 5-min water discharge data and turbidity recordings converted to concentrations by the two regressions, amounted to 655000 tonnes. The most likely explanation for the need for two regression equations for the two phases is differences in grain-size distribution causing differences in the turbidity recorded for the same sediment concentration (cf. Gilvear and Petts, 1985). With differences in grain-size distribution during the two phases, there would be different rating curves during the two phases. This conclusion is supported by investigations of grain-size distributions during the flushing of the Cachi reservoir in 1993 (Hydroconsult, 1995a). Four grain-size distribution curves of samples from the rapid phase and three curves from the free-flow phase at El Congo indicated that grain-size distributions were relatively fine-grained in the beginning of the rapid phase. During the following period, conditions varied but generally the material became coarser, which was especially evident in the last part of the free-flow phase (Hydroconsult, 1995a). Differences in grain size are probably the main reason for obtaining two different relationships, although a contributing explanation might be that the sampler is difficult to immerse deeply into the river during the very high water velocities of the rapid phase. Hence, some underestimation of the sediment concentration is probable during the rapid phase.

Accurate water discharge estimates are also of great importance for the accuracy of load calculations. Erosion of the cross-section during the rapid phase, and deposition during parts of the free-flow phase, may have given rise to differences in discharge for fixed water levels. The resulting effects on sediment transport calculations during the flushing are difficult to establish.

Moreover, a small amount of the material measured at El Congo comes from the Birris River basin downstream of the reservoir during the flushing period (Figure 1). This material is assumed to be of the same order of magnitude as the deposition of flushed material along the river banks and in the river channel from the dam to the measuring station El Congo. The river is steep here, and a large part of these deposits is coarse material. Deposition on river banks from the dam to El Congo has been investigated by Brandt (1999) and Brandt and Swenning (1999).

## FINAL ANALYSIS OF RESULTS

The final analysis of results is divided into three sub-headings. The depositional and flow conditions in the reservoir are first analysed from an empirical point of view. Deposition and throughflow are then analysed from a deterministic point of view based on mathematical modelling. Finally, a sediment budget is presented.

### *Flow conditions and deposition pattern based on empirical data*

*Density currents.* During field investigations of the reservoir, it was concluded that inflowing water often descends below the clearer water of the reservoir. Theoretical considerations confirmed that density currents are frequent and play a major role for the transportation and deposition processes in the

reservoir. Later measurements of temperature and turbidity differences within the Cachi Reservoir have verified the high frequency of density currents (Hydroconsult, 1995a,b). These measurements also indicated a rapid deposition in the upstream part of the main basin of the reservoir, probably concentrated in the former thalweg.

From geomorphological observations of the sedimentation surveys made in the reservoir, it was possible to estimate the approximate size of the density currents (cf. below). The depth and width of density currents were later used in the mathematical modelling.

*Upper basin.* The studies from map and photo interpretation of delta accumulation indicated an average annual net deposition of about 200000 m<sup>3</sup>. However, the deposition in the upper basin was high during the initial years, decreasing with time and with diminishing water volume in the basin. The present-day net deposition was estimated to amount to about 100000 m<sup>3</sup> per year in the upper basin, with an equivalent increase of deposition in the main basin (Sundborg and Jansson, 1992). Erosion from the upper basin was of the order of 60000 tonnes according to an approximate estimation in the field during flushing of the reservoir, complemented with photos of the upper basin, and some echo-sounding data (Sundborg, 1992d; Sundborg and Jansson, 1992).

*The thalweg in the main basin.* The sonograph map of the reservoir bottom, produced by the side-scan sonar, showed a distinct difference in grey level between the thalweg and the terraces around it. The higher gas content in the thalweg suggested a higher accumulation rate, and the thalweg was therefore interpreted as the route of density currents. The affected area is practically identical with the bankfull discharge area of the former river, the depth of which is 5 m as observed on the echo-sounder recordings. A few terraces below 5 m are partly affected by the same grey tone as the thalweg, and therefore the density currents were interpreted to be about 5 m and of underflow type.

Because of gas in the sediments, the stratigraphy could not be satisfactorily investigated by echo-sounding, or with the sub-bottom profiler. However, at the depth survey after the flushing, some thalweg sediments close to the dam were acoustically transparent, which indicates that they represented a water-sludge type of deposit with very low density.

The distribution of depths in the thalweg in the surveyed area on the two echo-sounding occasions is shown in Figure 7 (for location cf. Figure 2). The reason for the measured erosion pattern of Figure 7 becomes clear when comparing with the water-level curve. In May 1990, the water level was at the minimum generation level, 960 m a.s.l. (Figure 6). During the receding of the water level, material will have been re-eroded and transported in the thalweg down to a few metres below the water level, giving a thick deposit near the lower end of the regulation interval. As the water level slowly rose, the delta deposition gradually retreated. Between the end of flushing and the second depth survey, the water level was constantly high, and thus much of the deposition will have taken place in the upper basin, and in the upper parts of the main basin.

The X-rayed sediment cores from the old river channel contained a mixture of harder and softer layers, reflecting variations in stream power (Figure 5). The grain sizes of the newly deposited sediments decreased, as expected, in a downstream direction with fine sand and coarse silt dominating in channels on the delta plain, while clayey silt and silty clay material dominated on the downstream terraces, and in the downstream part of the old channel (Figure 9). The average dry bulk density of the thalweg sediments was found to be about 0.4 tonnes m<sup>-3</sup> (Axelsson, 1992a).

*Terraces.* The acoustical instruments seem to indicate that there are three possible developments on terraces during a flushing cycle. In brooks, the flushing has some eroding effect, while on flat surfaces the change is either negligible, or distinctly positive. During the slow phase, the flushing can not really cause much erosion on terraces in the live storage, both because the water velocity is too low, and because the sediments have dried up when being exposed during the preceding dry season. Instead, water hyacinths may become stranded, probably giving rise to an increased sedimentation when sediments are caught in the organic matter. If this does not occur, the sediments will become somewhat compacted due to drying up, and the thickness of sediment deposited during a year will not be very great (Erlingsson, 1992b).

From the X-ray radiographic analyses it was found that the silty and clayey deposits on the old river terraces of the reservoir show a rhythmic variation between hard mud crusts formed during subaerial

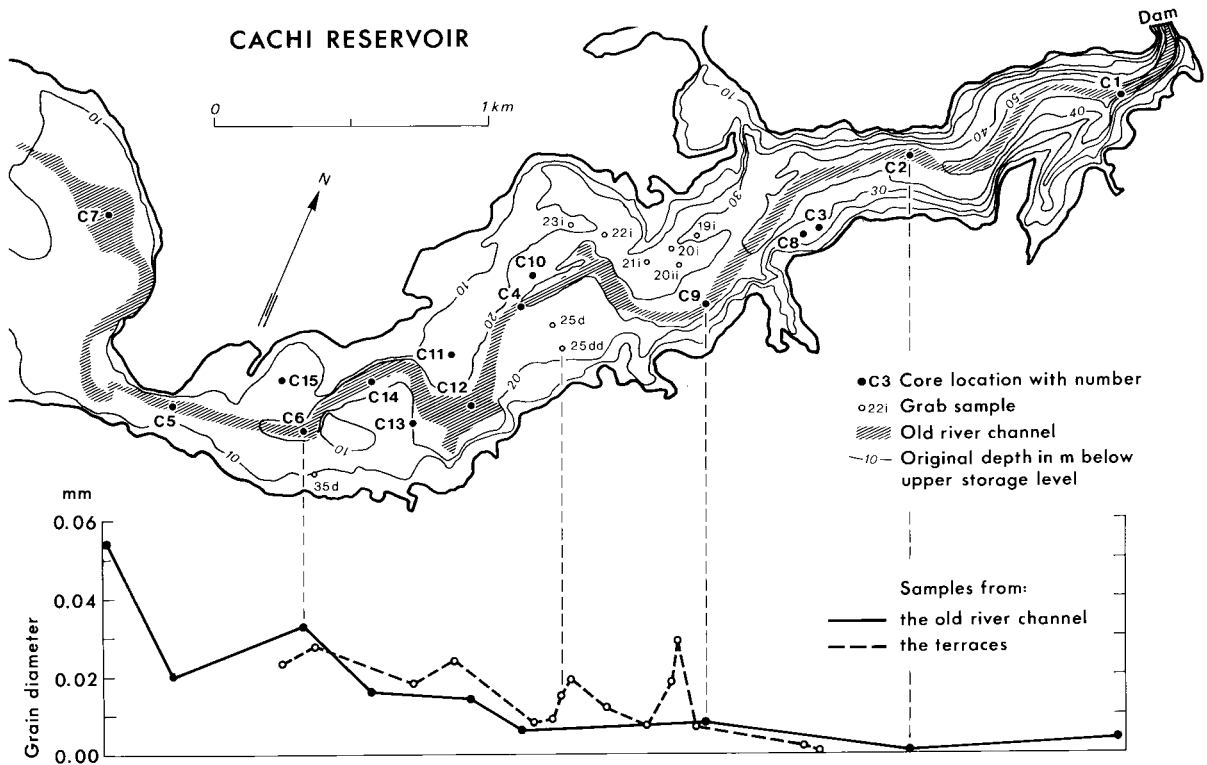


Figure 9. Location of cores and grab samples. Median particle sizes of surface sediment (from Axelsson, 1992a)

exposure, and softer layers. The deposits on the terraces are deposited under flow conditions without density currents, or from dispersed density currents.

From the measurements in pits dug on the terraces, it was found that 1.036 million  $\text{m}^3$  of material was deposited on a total terrace area of 1.027  $\text{km}^2$  during 19 years. Using a mean dry bulk density of 0.7  $\text{g cm}^{-3}$  for the whole depth of the vertical, as calculated from X-ray radiographic analysis, the corresponding weight is 38000 tonnes of solids per year deposited on terraces. The year-to-year variation is not very large, which justifies using this average in the sediment budget as 'net deposition on terraces' (i.e. during one hydrological year).

*Remaining areas (slopes and tributary mouths).* The rest of the reservoir area is made up of rather steep slopes, where the result of the depth surveys is meaningless due to a too-large inaccuracy of the position data. However, due to their steepness, the slopes are not expected to accumulate any significant amount of sediments, and the sub-bottom profiles seem to confirm this assumption (e.g. Erlingsson, 1992a, figure 9.9). On the other hand, the foot of the slopes may be expected to receive sediments from the slopes by gravity. Terrace brooks, which have been identified as efficient eroding agents during flushing, are located at the terrace foot.

Part of the material deposited on terraces and in tributary mouths was eroded during flushing. The erosion in the main basin of material deposited before flushing was estimated to amount to 320000 tonnes. The erosion in the thalweg was estimated to reach 219000 tonnes. The difference is 101000 tonnes, eroded mainly from the tributary mouths and from the brooks on the terraces.

#### *Deposition and throughflow based on modelling*

The mathematical modelling of sedimentation in the reservoir is based on the conclusions on flow conditions drawn above. The density current dimensions established above were used in the model as values for width and depth of active flow, during those flow conditions. Calculations were made for an

Table III. Reservoir deposition and sediment discharged through the reservoir, 'throughflow', estimated through mathematical modelling of the hydrological years 1980–1990

Sediment distribution	$\times 10^3$ tonnes year <sup>-1</sup>	%
Throughflow material	148	18.3
Deposited from turbidity currents	432	53.5
Deposited from flows without turbidity currents	167	20.7
Deposited bed load	60	7.5
Deposition and throughflow during one hydrological year	807	100

average hydrological year without any flushing of the reservoir, and were based on the mean annual suspended sediment inflow during the 1980–1990 period of 747000 tonnes, and 60000 tonnes of estimated bed load. The results are indicated in Table III (from Sundborg and Jansson, 1992). The trap efficiency was 80% of the suspended sediment inflow, and 82% of the total sediment inflow (Table III). The throughflow material, i.e. the material that flows through the whole reservoir without deposition, amounted to 20% of the suspended sediment inflow. Of the material deposited from flows without turbidity currents, some is deposited in the upper basin, some on terraces, and some in the old channel.

The mathematical modelling of the present investigation period indicated a suspended sediment deposition of 110000 tonnes in the upper basin up until the main erosion phase of the flushing, September 20, 1990.

#### *Sediment budget*

The sediment budget of the Cachi reservoir covers the period between the ends of two reservoir flushings (Table IV). The budget is divided into three parts, each representing the same sediment amount accounted for in different ways. Part A accounts for the credit side of the balance sheet, that is to say the sediment inflow to the reservoir. Parts B1 and B2 account for the debit side of the balance sheet in two different ways.

*Part A. Sediment inflow to the reservoir.* The water discharge and sediment concentration is frequently high during the more rainy season (from May to the first part of December) at both Palomo and La Troya, which explains why sediment load is high during that period (cf. Figure 3). The sediment load at La Troya amounted to *c.* 200000 tonnes, both when calculated with a sediment rating curve, and when using turbidimeter recordings most of the time. Thus, it must be considered a reasonably reliable figure. The uncertainty was estimated to be  $\pm 15\%$ . October 12–13, with very high water stages, and another 5 days, October 1–5, are not included in this figure. The load of October 1–5 and October 12–13 is probably of the order of 65000 tonnes  $\pm 75\%$ . The large error margin is due to the great uncertainty in the discharge calculations caused by erosion of the banks of the gauging station. The combined uncertainty for the whole period was calculated to be 22% (Table IV).

There was considerable river bank erosion downstream of the measuring station on October 11–13, when also the pump house was washed away (cf. Figure 3). A large part of the bank material was coarse with many boulders. Of the 40000 tonnes of estimated bank erosion, only some 20% were considered to be routed down to the reservoir during the short period before the end of the flushing. Thus, the mass of material ending up in the reservoir was estimated to be roughly 8000 tonnes.

The sediment load at Palomo was calculated with sediment rating curves and amounted to about 450000 tonnes. To this figure must be added about 28000 tonnes from the dredging of the El Llano reservoir, and construction works in the area downstream of Palomo. The suspended sediment transport past Palomo is uncertain for the whole period because of problems in converting the turbidity recordings to sediment concentrations at high water discharges. The uncertainty is estimated to be 30% (Table IV).

The load from the unsampled area was estimated by comparison with a neighbouring basin. The erosion conditions of the unsampled area are similar to the erosion conditions of the drainage basin

Table IV. Sediment budget for the period September 16, 1989 to October 13, 1990<sup>a</sup>

	× 10 <sup>3</sup> tonnes	Estimated uncertainty (%)	Uncertainty, × 10 <sup>3</sup> tonnes
<b>A. Sediment inflow</b>			
Suspended load			
Past La Troya	265	±22	58
Past Palomo	450	±30	135
Dredged from El Llano and construction works	28	±10	3
From unsampled area	110	±50	55
Bank erosion at and downstream of La Troya	8	±100	8
<i>Total</i>	861	±18	157
Bed load	66	±50	33
<b><i>Grand total</i></b>	<b>927</b>	<b>±17</b>	<b>161</b>
<b>B1. Sediment erosion, throughflow, and net deposition</b>			
Eroded material			
Main basin	320	±24 <sup>b</sup>	77
Upper basin	60	±50	30
<i>Total</i>	380	±22	82
Throughflow			
Before September 4	115	±40	46
Inflow and outflow after September 4 <sup>c</sup>	301	±30	90
<i>Total</i>	416	±24	101
Net deposition			
Upper basin	95	±50	48
On terraces	38	±20	8
<i>Total</i>	133	±36	48
<b><i>Grand total</i></b>	<b>929</b>	<b>±15</b>	<b>139</b>
<b>B2. Sediment outflow and net deposition</b>			
Outflow			
Throughflow before September 20, 1990	133	±40	53
Sediment flushed past El Congo	653	±20	131
Bed load	10	±100	10
<i>Total</i>	796	±18	141
Net deposition			
Upper basin	95	±50	48
On terraces	38	±20	8
<i>Total</i>	133	±36	48
<b><i>Grand total</i></b>	<b>929</b>	<b>±16</b>	<b>149</b>

<sup>a</sup> The budget is divided into one 'credit' part, and two alternative 'debit' parts, each accounting for the same amount of sediments in different ways. The uncertainties in the values are all estimated with one exception. Total uncertainties are calculated as the square root of the sum of squared uncertainties in tonnes.

<sup>b</sup> This uncertainty has been analysed in the article. All other uncertainties are estimated.

<sup>c</sup> Of the 310 000 tonnes of sediment inflow after September 4, 9000 tonnes were deposited on terraces or in the upper basin.

upstream of La Troya. Since the surface area is half of that upstream of La Troya, the load is estimated to be 110000 tonnes, which is half the load at La Troya minus 45000 tonnes of waste load from a factory in the Navarro basin. The bed load inflow is estimated to amount to 8% of the suspended load except for the El Llano material, that is to say 66000 tonnes of bed load from the whole area (Table IV).

*Part B1. Sediment erosion, throughflow, and net deposition.* The erosion in the main basin of material deposited from the end of the flushing in 1989 up to the first depth survey on September 4, 1990, was calculated from echo-soundings to be 320000 tonnes  $\pm$  24%. Erosion from the delta area of the upper basin was estimated to be of the order of 60000 tonnes.

The sediment throughflow during the period from the previous flushing to the first depth survey, was determined by modelling to be *c.* 20% of the suspended sediment inflow of 573000 tonnes, that is 115000 tonnes.

About 280000 tonnes of suspended load, 22000 tonnes of bed load, plus 8000 tonnes of eroded bank material, entered the reservoir during the period between the first depth survey and the end of the flushing. Some of this sediment was temporarily deposited in the reservoir, but most of it was eroded again during the flushing. All material entering the reservoir during the rapid phase of the flushing passed the reservoir. Therefore, all the sediment entering the reservoir after the first depth survey of September 4 was counted as throughflow in the budget, less 9000 tonnes. This was deposited on accumulation surfaces before the main erosion phase of the flushing, beginning on September 20.

The sediment net deposition in the upper basin indicated in Table IV was calculated as follows: the mathematical modelling indicated a suspended sediment deposition of 110000 tonnes in the upper basin. The bed load deposition in the upper basin was estimated to be 45000 tonnes up to the erosion phase of the flushing. As mentioned above, the erosion in the upper basin was estimated to be 60000 tonnes. The net deposition in the upper basin is then the difference, 95000 tonnes.

The net deposition on terraces was 38000 tonnes measured as a mean value for a 19-year period. There is no reason for a very different net deposition this year.

*Part B2. Sediment outflow and net deposition.* The mathematical modelling indicated that the trap efficiency was about 80% of the suspended sediment inflow, and thus, that about 20% of the incoming suspended sediment were discharged straight through the reservoir. The inflow of suspended sediment up to the beginning of the erosion phase of the flushing on September 20, 1990, was 664000 tonnes. Consequently, the sediment throughflow was calculated to be  $0.2 \times 664000$  tonnes = 133000 tonnes.

The suspended sediment outflow during flushing, used in the budget, was calculated from water sample concentrations at El Congo. During the passage of water peaks of the slow flushing phase, the load amounted to 27000 tonnes. During the rapid phase the load was 279000 tonnes, and during the free-flow phase 347000 tonnes; altogether 653000 tonnes. This value also includes some coarse material that formerly may have been transported as bed load.

Only part of the bed load deposited in the braided river system of the upper basin was transported out of the reservoir, because only one channel was deeply eroded in the upper basin during flushing. Part of the bed load deposited by tributaries directly into the reservoir was also evacuated during flushing. From these considerations, it was estimated that 10000 tonnes left the reservoir as bed load, making a total sediment outflow during flushing of 663000 tonnes.

The final phase of the flushing in 1990 took place during heavy rains and high discharges in contributing rivers. This helped to make the evacuation of the channels of the reservoir complete in 1990. There might even have been a slight net erosion in the old channels of the reservoir, of material left in the reservoir from the flushing in 1989. In that case, the sediment outflow might have been greater than the inflow to the reservoir this year. The uncertainty of the sediment load flushed past El Congo is estimated to be  $\pm$  20% of the 653000 tonnes. Most of this uncertainty relates to the deposition of flushed material, or the entrainment of additional material coming from tributaries, between the dam and El Congo during the flushing.

*Budget uncertainties.* A statistical uncertainty assessment of the measurements and calculations was only performed for the bathymetric measurements. For other values, the uncertainties are estimated based on knowledge of sedimentation processes, in combination with measurement and calculation methods.

The ideal measurement situation is that the instrument measures the very property of interest. If random errors are too large, one can simply make more observations. In this paper, the measurement of sediment bulk density comes close to that ideal. The accuracy of the mean dry bulk density is much better than  $\pm$  10% for the part of the population that was sampled. However, only the top 50 cm could be sampled, and the density below had to be extrapolated.



Instrument resolution and accuracy may be a very small part of the true uncertainty. In effect, it might be next to irrelevant in cases where the vast majority of the uncertainty is introduced through various conversions; i.e. in situations where one can not measure the property of interest directly, but has to resort to conversions. If regressions are developed and used for a whole measurement series, the uncertainty of that may completely overshadow other errors.

In the calculation of sediment transport in rivers, there are several steps of conversions between measurement data and final results: Water velocity is converted to discharge by multiplication with the cross-section area to develop a discharge rating curve; water level is then converted to discharge by using this rating curve; turbidity recordings are converted to sediment concentrations using a conversion regression determined from water sample concentrations; discharge values are converted to sediment load by using a sediment rating curve. Each of these steps increases the uncertainty.

Measurements should be unbiased. Water sampling, e.g. should be unbiased as regards water discharges. Especially at Palomo the accuracy of the sediment load was mostly a matter of sampling strategy. Sampling of a large number of high-water events at Palomo resulted in a sediment rating curve that yielded three times higher load compared with the old rating curve, which was based on data sampled in the mornings. Turbidimeters were of great help in obtaining concentration data from the passage of high-water events, especially as they occur in the afternoons and at night. On the other hand, the main source of error in the sediment load at Palomo, with the present sampling strategy, lies in the conversion of the turbidity values to concentrations because of the low number of water samples at high turbidity. The use of hourly discharges, instead of mean daily discharges, was only responsible for an increase in load estimate of 20–30%.

Another problem, which is more difficult to address, is changing cross-sections during those high flows when sediment transport is the largest. As long as one depends on sampling and *in situ* measurements, high-water events causing bed and bank erosion will continue to be a problem.

A general reflection is that we seem to overestimate the uncertainty in estimated values when based on professional experience, 'to be on the safe side', and we seem to intuitively underestimate the uncertainty of computer-calculated values. Erlingsson and Jansson (1999) calculated the uncertainty of the bathymetric survey in two different ways, and got results with empirical data quite similar to those obtained with analytical data. The estimated uncertainties reported in the present paper are offered as an indication of the relative degree of uncertainty of the calculated or estimated values in the budget and the main causes of the uncertainties are mentioned.

Because independent measurements and different methods are used to calculate the various components of the sediment budget, the credit and debit sides of the budget can be checked against each other. The total turnover of sediments is thus probably estimated to be well within  $\pm 10\%$ .

## SUMMARY AND CONCLUSIONS

For sustainable long-term use of some reservoirs, it is necessary to manage the sediments. Scour valve release of the Cachí reservoir has successfully been undertaken to remove deposited sediment. However, efficiency in flushing operations in other reservoirs requires knowledge of inflow conditions as well as flow and sedimentation conditions within those particular reservoirs. The recommendations must therefore be to investigate those conditions.

The Cachí reservoir is flushed nearly every year to release sediments. The aim of this study was to determine the sediment inflow, the flow and sedimentation conditions in the reservoir, and the sediment outflow. Independent measurements and methods were used for sediment calculations, which were combined into a sediment budget for the reservoir.

The flushing of the Cachí reservoir was found highly effective in releasing sediment. Of the sediment inflow of *c.* 930000 tonnes during the investigation period, there was a sediment throughflow of 133000 tonnes (14.3%) up to the beginning of the flushing, which corresponds to a throughflow of 20% of the suspended sediment inflow during that time. The sediment outflow during flushing was *c.* 665000 tonnes

(71.4%), and the net accumulation in the reservoir was 133000 tonnes (14.3%). It was found that the reasons for the efficient sediment release were the flow and depositional conditions in the reservoir, and its morphology with a deep channel. Density currents are formed due to temperature and concentration differences between the inflowing water and the surface water of the reservoir. Therefore, most of the deposition takes place in the old river channel of the reservoir, which is also where most erosion takes place during the final flushing phases.

The flushing efficiency indicated above can be compared with calculations from the bathymetric survey. About 513000 tonnes had accumulated until the in-survey on September 4, to be compared with 380000 tonnes of erosion of that material during the flushing. Thus, 74% of the accumulated sediments were eroded.

Although some budget components have large estimated or calculated uncertainties, the credit side and the two debit sides of the sediment account have total uncertainties around  $\pm 17\%$ . This circumstance, and the fact that the budget is balanced, help to validate that the sediment budget is viable, and make it probable that the major components of the sediment budget are of the right order of magnitude.

The goal of obtaining correct values of sediment transport in small flashy rivers by using sediment rating curves was achieved by collecting data from a large number of high-water events at equal intervals during their rising and falling stages. This was attained by using turbidimeter measurements. Sediment rating curves were developed as linear regressions on logged mean loads in discharge classes.

The volume of material eroded in the reservoir during flushing was determined from echo-soundings before and after the flushing. Steps have been taken to prevent small systematic errors, which are a more serious problem when volume change is sought. An error analysis indicated that the uncertainty of the measured average depth of erosion was  $\pm 0.045$  m or 16% of the measured erosion depth of 0.280 m. Even though each individual grid cell value had a rather large uncertainty, the great number of grid cells effectively masked that in the calculation of the average. After adjustments for unmeasured area, post-flushing deposition, and sediment density, the material deposited in the main basin until September 4 and eroded during flushing was calculated at 320000 tonnes  $\pm 24\%$ .

Dry bulk densities of reservoir deposits are often overestimated. Accuracy in determining the dry bulk density of the reservoir deposits was of major significance for a correct sediment budget of the Cachí reservoir. X-ray radiographic and densitometric analysis was found to be an accurate method to determine the density. The X-ray analyses indicated a dry bulk density of 0.4 tonnes  $\text{m}^{-3}$  of the loose material in the thalweg and 0.7 tonnes  $\text{m}^{-3}$  of the whole deposition depth on the terraces.

Sundborg's physically based mathematical model was used to determine the trap efficiency and throughflow of the reservoir, amounting to 80% and 20% of the suspended sediment inflow, respectively.

The sediment outflow during flushing was measured at a station downstream of the reservoir. The measurements were carefully planned with frequent water sampling, and were found satisfactory, with reservation for some problems in depth-integrated water sampling at high flow velocities and turbid water.

Experiences gained during the work suggest that one should take care not to be over-confident with the precision of calculated results. One can hardly over-emphasize the importance of a correct sampling strategy. A statistical analysis of the uncertainty is a valuable tool to decrease the costs of gathering adequate data to achieve the required precision.

#### ACKNOWLEDGEMENTS

This project would not have been possible without good co-operation with ICE. The Costa Rican team did most of the instrument installations, measurements, and laboratory work. Among the many persons in the Costa Rican team, the authors want especially to thank Alexis Rodríguez, Carlos Ramírez, Luis Acuña, and Alexia Pacheco. The project was a joint teamwork within the Swedish group consisting of Åke Sundborg, Valter Axelsson, Margareta Jansson, and Ulf Erlingsson. Per-Olof Hårdén helped with the turbidimeter installations. Professor Åke Sundborg was responsible for mathematical modelling, and delta development estimations, and Professor Valter Axelsson was responsible for X-ray radiographic analyses.

## REFERENCES

- Axelsson V. 1967. The Laitaure delta. A study of deltaic morphology and processes. *Geografiska Annaler* **49A**(1): 1–27.
- Axelsson V. 1979. Sjöars sediment studeras med röntgenteknik. (Lake deposits are studied by X-ray technique). *Ymer* **99**: 133–144.
- Axelsson V. 1992a. X-ray radiographic analyses of sediment cores from the Cachi reservoir. In *Sedimentological Studies in the Cachi Reservoir, Costa Rica, UNGI Rapport 81*, Jansson MB, Rodríguez A (eds). Department of Physical Geography, Uppsala University: Uppsala; 89–99.
- Axelsson V. 1992b. X-ray radiographic techniques in studying sedimentary properties and reservoir sedimentation. A manual, Appendix 2, *UNGI Rapport 81*; 196–217.
- Axelsson V, Hårdén P-O. 1987. Computer controlled radiographic sediment analyses, Department of Physical Geography, Uppsala University, Unpublished Report.
- Brandt SA. 1999. Reservoir desiltation by means of hydraulic flushing: Sedimentological and geomorphological effects in reservoirs and downstream reaches as illustrated by the Cachi reservoir and the Reventazón river, Costa Rica, *Thesis*, Geographica Hafniensia A8, Publications, Institute of Geography, University of Copenhagen.
- Brandt SA, Swenning J. 1999. Sedimentological and geomorphological effects of reservoir flushing: the Cachi reservoir, Costa Rica, 1996. *Geografiska Annaler* **81A**(1): 391–407.
- Brandt A, Strömbäck N, Swenning J. 1995. Downstream sedimentological effects of the 1993 flushing of the Cachi reservoir, Costa Rica, MSc Thesis, Institute of Earth Sciences, Uppsala University.
- Bruk S. 1985. Methods of computing sedimentation in lakes and reservoirs. A contribution to the International Hydrological Program, IHP, Project A.2.6.1, UNESCO (with contributions by Evrad, McManus, Jobson, Fan Jiahua and Bruk (eds)).
- Cortes VM, Oconitrillo G, Brenes LG. 1987. Calculo de tasas de erosión hídrica en Cot y Tierra Blanca de Cartago, Informe final proyecto de investigación 214-85-083. Departamento de Geografía, Universidad de Costa Rica.
- Eriksson E. 1972. On design and operation of hydrologic networks. *Nordisk Hydrologisk Konferanse 1972, Sandefjord*, 285–301.
- Erlingsson U. 1990. Geomorphological development of the bottoms off Österlen, southernmost Sweden, *UNGI Rapport 76*; 136 pp.
- Erlingsson U. 1992a. Survey with side-scan sonar and sub-bottom profiler. In *Sedimentological Studies in the Cachi Reservoir, Costa Rica, UNGI Rapport 81*, Jansson MB, Rodríguez A (eds). Department of Physical Geography, Uppsala University: Uppsala; 101–110.
- Erlingsson U. 1992b. Repeated depth soundings. In *Sedimentological Studies in the Cachi Reservoir, Costa Rica, UNGI Rapport 81*, Jansson MB, Rodríguez A (eds). Department of Physical Geography, Uppsala University: Uppsala; 111–118.
- Erlingsson U, Jansson MB. 1999. Integrated study of reservoir flushing efficiency, *Hydropower into the Next Century III*, Conference Proceedings, Gmunden, Austria, 18–20 October 1999; 737–746.
- Ferguson RI. 1986. River loads underestimated by rating curves. *Water Resource Research* **22**(1): 74–76.
- Gilvear DJ, Petts GE. 1985. Turbidity and suspended solids variations downstream of regulating reservoir. *Earth Surface Processes and Landforms* **10**: 363–373.
- Heidel SG. 1956. The progressive lag of sediment concentration with flood waves. *Transactions of the American Geophysical Union* **37**(1): 56–66.
- Helsel DR, Hirsch RM. 1992. *Statistical Methods in Water Resources. Developments in Water Science Series*. Elsevier: Amsterdam.
- Hydroconsult. 1995a. *Sedimentation and Erosion Processes Related to the Hydropower Projects Angostura, Guayabo and Siquirres. Part 1*. Hydroconsult: Uppsala, Sweden. ISBN 91-88476-02-2.
- Hydroconsult. 1995b. *Sedimentation and Erosion Processes Related to the Hydropower Projects Angostura, Guayabo and Siquirres. Appendix 2: Studies of Sediment Transport Conditions in the Cachi Reservoir*. Hydroconsult: Uppsala, Sweden.
- Jansson MB. 1985. A comparison of detransformed logarithmic regressions and power function regressions. *Geografiska Annaler* **67A**(1–2): 61–70.
- Jansson MB. 1992a. Suspended sediment inflow to the Cachi reservoir. In *Sedimentological Studies in the Cachi Reservoir, Costa Rica, UNGI Rapport 81*, Jansson MB, Rodríguez A (eds). Department of Physical Geography, Uppsala University: Uppsala; 41–77.
- Jansson MB. 1992b. Suspended sediment outflow from the Cachi reservoir during the flushing in 1990. In *Sedimentological Studies in the Cachi Reservoir, Costa Rica, UNGI Rapport 81*, Jansson MB, Rodríguez A (eds). Department of Physical Geography, Uppsala University: Uppsala; 127–136.
- Jansson MB. 1992c. Turbidimeter measurements in a tropical river, Costa Rica. *IAHS Publication* **210**: 71–78.
- Jansson MB. 1996. Estimating a sediment rating curve of the Reventazón river at Palomo using logged mean loads within discharge classes. *Journal of Hydrology* **183**: 227–241.
- Jansson MB, Rodríguez A (eds). 1992. *Sedimentological Studies in the Cachi Reservoir, Costa Rica, UNGI Rapport 81*. Department of Physical Geography, Uppsala University: Uppsala.
- Lane EW, Borland WM. 1951. Estimating bed load. *Transactions of the American Geophysical Union* **32**(1): 121–123.
- Leeks GJL, Newson MD. 1989. Responses of the sediment system of a regulated river to a scour valve release: Llyn Clywedog, Mid-Wales, UK. *Regulated Rivers: Research and Management* **3**: 93–106.
- McCann C, McCann DM. 1969. The attenuation of compressional waves in marine sediments. *Geophysics* **34**(6): 882–892.
- Morris GL, Fan J. 1997. *Reservoir Sedimentation Handbook. Design and Management of Dams, Reservoirs, and Watersheds for Sustainable Use*. McGraw-Hill: New York. 805 pp.
- Nilsson B. 1971. Sedimenttransport i svenska vattendrag, Ett IHD-projekt. Del1: Metodik, *UNGI Rapport 4*, Uppsala (in Swedish).

- Ramírez C, Zeledón R, Rodríguez A. 1992. Deposition and general sediment distribution in the Cachi reservoir. In *Sedimentological Studies in the Cachi Reservoir, Costa Rica, UNGI Rapport 81*, Jansson MB, Rodríguez A (eds). Department of Physical Geography, Uppsala University: Uppsala; 79–88.
- Rodríguez A, Jansson MB (eds). 1992. *Estudios Sedimentológicos en el Embalse Cachi. Afluencia de Sedimentos, Sedimentación del Embalse y Efectos de los Desembalses. Departamento de Geografía Física. Universidad de Uppsala: Uppsala; pp. 228.*
- Sundborg Å. 1992a. Sedimentation in the Cachi reservoir illustrated by mathematical modelling. In *Sedimentological Studies in the Cachi Reservoir, Costa Rica, UNGI Rapport 81*, Jansson MB, Rodríguez A (eds). Department of Physical Geography, Uppsala University: Uppsala; 137–156.
- Sundborg Å. 1992b. Reservoir sedimentation. A manual. Appendix 1. In *Sedimentological Studies in the Cachi Reservoir, Costa Rica, UNGI Rapport 81*, Jansson MB, Rodríguez A (eds). Department of Physical Geography, Uppsala University: Uppsala; 171–193.
- Sundborg Å. 1992c. Delta development. In *Sedimentological Studies in the Cachi Reservoir, Costa Rica, UNGI Rapport 81*, Jansson MB, Rodríguez A (eds). Department of Physical Geography, Uppsala University: Uppsala; 82–83.
- Sundborg Å. 1992d. Erosion processes in the Cachi reservoir during the flushing period in 1990, *UNGI Rapport 81*, Department of Physical Geography, Uppsala University, Uppsala, 119–126.
- Sundborg Å, Jansson MB. 1992. Present and future conditions of reservoir sedimentation. In *Sedimentological Studies in the Cachi Reservoir, Costa Rica, UNGI Rapport 81*, Jansson MB, Rodríguez A (eds). Department of Physical Geography, Uppsala University: Uppsala; 157–164.
- Walling DE. 1977a. Limitations of the rating curve technique for estimating suspended sediment loads, with particular reference to British rivers. *IAHS Publication* **122**: 34–48.
- Walling DE. 1977b. Assessing the accuracy of suspended sediment rating curves for a small basin. *Water Resources Research* **13**(3): 531–538.
- Walling DE, Webb BW. 1981. The reliability of suspended sediment load data. *IAHS Publication* **133**: 177–194.
- White WR. 1990. Reservoir sedimentation and flushing, *Conference Proceedings, International Conference on Water Resources in Mountainous Regions*, Lausanne, Switzerland, August 27–September 1, 1990. Reproduced by HR Wallingford, UK.